Applied Catalysis B: Environmental 136–137 (2013) 103–111

Contents lists available at SciVerse ScienceDirect

Applied Catalysis B: Environmental

journal homepage: www.elsevier.com/locate/apcatb

A cyclic reaction pathway triggered by ammonia for the selective catalytic reduction of NO_x by ethanol over Ag/Al_2O_3

Yunbo Yu*, Jiaojiao Zhao, Yong Yan, Xue Han, Hong He

Research Center for Eco-Environmental Sciences, Chinese Academy of Sciences, Beijing, 100085, China

ARTICLE INFO

Article history:
Received 28 November 2012
Received in revised form 26 January 2013
Accepted 29 January 2013
Available online 6 February 2013

Keywords:
Selective catalytic reduction of NO_x
Ammonia
Enolic species
Ag/Al_2O_3
Isocyanate

ABSTRACT

Alumina-supported silver catalysts (Ag/Al_2O_3) prepared using nordstrandite as a precursor exhibited excellent activity for the selective catalytic reduction of NO_x by ethanol (ethanol-SCR). During the ethanol-SCR, the formation of NH_3 was observed over all Ag/Al_2O_3 catalysts, the amount of which was related to silver loading, reaction temperature, and the concentration of ethanol used, even when water was excluded from the inlet gas. Transient activity testing and in situ diffuse reflectance infrared Fourier transform spectroscopy (DRIFTS) analysis showed that the reaction between isocyanate species (–NCO) and water is the main pathway of NH_3 formation. Addition of NH_3 enhanced the NO_x conversion for ethanol-SCR and the oxidation of ethanol over 3 wt% Ag/Al_2O_3. DRIFTS analysis revealed for the first time that NH_3 reacted with enolic species to form –NCO over Ag/Al_2O_3, thus resulting in a novel and cyclic reaction pathway for ethanol-SCR.

1. Introduction

Nitrogen oxides (NO_x) cause a variety of health and environmental impacts, such as the formation of photochemical smog and acid rain. Consequently, NO_x removal has become an important issue for environmental protection. The diesel engine has the advantages of low fuel consumption and low emissions of CO_2, CO, and HC, while NO_x removal is one of the major challenges for its commercial application. Among the NO_x reduction technologies being developed to control diesel engine emissions, selective catalytic reduction by hydrocarbons (HC-SCR) has attracted much attention as a possible alternative to urea/NH_3-SCR, the latter of which has been commercially used in Europe, the United States, and Japan [1–5].

Hitherto, numerous catalysts such as zeolitic oxide, base metal/oxide and noble metal catalysts have been found to be effective for the HC-SCR of NO_x in the presence of excess oxygen [3,4,6–9]. Among them, γ-alumina-supported silver (Ag/Al_2O_3) is known as one of the most effective catalysts [10–17]. When using oxygenated hydrocarbons as reductants, particularly ethanol, Ag/Al_2O_3 shows high activity even in the presence of SO_2 and H_2O [18]. Over Ag/Al_2O_3, though NO_x was mainly converted to N_2, there was still an unexpected production of ammonia, the concentration of which varied with the silver loading of the catalyst, the Lewis acidity of the support, reaction temperature, water vapor, the employed reductant and its concentration [8,19,20]. During C_3H_6-SCR carried out by Meunier et al. [8], NH_3 selectivity was 5% on pure γ-Al_2O_3, which decreased to 3% over 1.2 wt% Ag/Al_2O_3, and further increasing the silver loading to 10 wt% resulted in the disappearance of NH_3. Miyadera [19] observed that the concentration of NH_3 increased with the amount of ethanol employed over 2 wt% Ag/Al_2O_3, and also increased with the growing space velocity. Moreover, a correlation between NH_3 yield and acidic surface properties of the alumina support was likewise established for ethanol-SCR over Ag/Al_2O_3, such that the selectivity of NH_3 varied between 6% and 27% at 723 K with increasing numbers of strong Lewis acid sites [20]. In addition, water vapor plays a crucial role in NH_3 formation, as confirmed by the result that the NH_3 concentration promptly increased from 10 to 90 ppm at 773 K over 2.0 wt% Ag/Al_2O_3 as soon as 10% H_2O was added into the feed gas of NO + ethanol + O_2 [19].

Since ammonia is one of the main basic species commonly present in the atmosphere, it readily reacts with strongly acidic species such as NO_x and SO_x, leading to smog formation. As a result, minimizing the release of ammonia during the HC-SCR process should be given much more attention. With this aim, it will be helpful to recall the mechanism of the reduction of NO_x by hydrocarbons.

Generally, HC-SCR of NO_x can be considered as follows: $NO + O_2 + HC \rightarrow NO_x$ (adsorbed nitrate in particular) + ad-$C_xH_yO_z \rightarrow$ R-ONO + R-$NO_2 \rightarrow$ –NCO + –CN $\rightarrow N_2$ [5,12,21]. Among the intermediates mentioned above, the isocyanate species (–NCO) was considered to be highly reactive toward NO + O_2 and/or surface

* Corresponding author. Tel.: +86 10 62849121; fax: +86 10 62849121.
E-mail address: ybyu@rcees.ac.cn (Y. Yu).

0926-3373/$ – see front matter © 2013 Elsevier B.V. All rights reserved.
http://dx.doi.org/10.1016/j.apcatb.2013.01.048

nitrates to produce N_2, and thus play a critical role in HC-SCR over Ag/Al_2O_3. Back in 1973, Unland [22] found that –NCO species adsorbed on the $Pt/A1_2O_3$ surface reacted with H_2O to yield NH_3 and CO_2. Such hydrolysis of –NCO on Ag/Al_2O_3 catalysts was further demonstrated by DRIFTS and mass spectrometry (MS) measurements [23].

As a reduced form of nitrogen, ammonia can react with oxidized species of this element (e.g. surface-bound nitrates, NO + O_2) to form the final product of N_2, thus ammonia has been regarded as a reactive intermediate for HC-SCR over Ag/Al_2O_3 [1,18,19,23]. However, as reported by Richter et al. [24], the Ag/Al_2O_3 catalyst was not active for NO_x reduction by NH_3 in the absence of H_2 (only reaching approximately 30% NO_x conversion at high temperature above 823 K), which was further confirmed by Kondratenko et al. [25] through a transient isotopic approach. Consequently, the intermediacy of NH_3 for the HC-SCR over Ag/Al_2O_3 needs to be further clarified.

In this study, γ-alumina-supported silver catalysts prepared using nordstrandite as a precursor were employed to evaluate their performance in the ethanol-SCR. Particular attention was paid on the formation of NH_3 and its role in the NO_x reduction process. Combined with the results of DRIFTS measurements, the intermediacy of NH_3 in ethanol-SCR was clarified. A novel reaction pathway concerning NH_3 participating in ethanol-SCR by reaction with enolic species over Ag/Al_2O_3 was proposed.

2. Experimental

2.1. Catalyst preparation

The precursor of γ-Al_2O_3 was synthesized by the following procedure. 4.8 g $Al(NO_3)_3$ was added into 100 mL distilled water under vigorous stirring, followed by dropwise addition of anhydrous ethylenediamine, adjusting the pH value of the solution to ~8.5. After stirring for another 2 h, the gel was covered by PE film and aged at 303 K for 12 h. To obtain the final product, the precipitate was separated from the solution by centrifuging, and then dried at 363 K in air for 12 h.

Ag/Al_2O_3 catalysts with different silver loadings were prepared by an impregnation method [13], immersing the support synthesized by the above procedure into an aqueous solution of silver nitrate. After impregnation, the excess water was removed in a rotary evaporator at 333 K, and then the product was calcined in air at 873 K for 3 h.

2.2. Catalyst characterization

Powder X-ray diffraction (XRD) measurements of the catalysts were carried out on a Rigaku D/max-RB X-ray Diffractometer (Japan) using CuKα radiation and operating at 40 kV and 40 mA. The patterns were taken over the 2θ range from 10° to 90° at a scan speed of 4° min^{-1}.

N_2 adsorption–desorption isotherms over the series of Ag/Al_2O_3 catalysts were obtained at 77 K using a Quantachrome Autosorb-1C instrument. Prior to N_2 physisorption, the catalysts were degassed at 573 K for 3 h. Surface areas were determined by the multi-point BET equation in the 0.05–0.35 partial pressure range. Pore volumes, average pore diameters and pore size distributions were determined by the Barrett–Joyner–Halenda (BJH) method from the desorption branches of the isotherms.

The morphology and the particle size distribution of the prepared samples were examined by transmission electron microscopy (TEM, HITACHI H-7500) with 80 kV acceleration voltage.

2.3. Activity test

The activity test was carried out in a fixed-bed reactor by passing a gaseous mixture of NO (800 ppm), NH_3 (150 ppm) (when added), C_2H_5OH (1565 ppm), O_2 (10%) and water vapor (10%) (when added) in N_2 balance at a total flow rate of 1000 mL min^{-1} (GHSV = 50,000 h^{-1}). An aqueous C_2H_5OH solution was supplied with a micropump and vaporized by a coiled heater. The concentrations of NO, NO_2, N_2O and NH_3 were analyzed on-line by an FTIR spectrometer (Nicolet is10) equipped with a gas cell of volume 0.2 dm^3. In this case, the gas cell of the FTIR spectrophotometer and the gas line were heated to 393 K to avoid water condensation. The spectra were collected with a resolution of 0.5 cm^{-1} and with an accumulation of 16 scans when the SCR process reached a steady state. The concentration of C_2H_5OH and CH_3CHO was monitored by periodically injecting the outlet gas into a gas chromatograph (Shimadzu, GC-2014C) equipped with two TCDs and one FID. In our case, the concentration of N_2O was negligible during the reduction of NO_x by ethanol over Ag/Al_2O_3. Based on this, NO_x conversion and N_2 (NH_3) selectivity were calculated by the following equations:

$$NO_x \text{ conversion}\,(\%) = \frac{[NO]_{in} - [NO + NO_2]_{out}}{[NO]_{in}} \times 100$$

$$N_2 \text{ selectivity}\,(\%) = \frac{[NO]_{in} - [NO + NO_2 + NH_3]_{out}}{[NO]_{in}} \times 100$$

$$NH_3 \text{ selectivity}\,(\%) = \frac{[NH_3]_{out}}{[NO]_{in}} \times 100$$

2.4. In situ DRIFTS measurement

In situ DRIFTS spectra were recorded on a Nexus 670 FT-IR (Thermo Nicolet), equipped with an in situ diffuse reflection chamber and a high sensitivity MCT/A detector. In this case, Ag/Al_2O_3 catalyst (3 wt%) was finely ground and placed in ceramic crucibles in the in situ chamber. Mass flow controllers and a sample temperature controller were used to simulate the real reaction conditions, such as mixture of gases, pressure and sample temperature. Prior to recording each DRIFTS spectrum, the sample was heated in situ in 10% O_2/N_2 flow at 823 K for 1 h, then cooled to the desired temperature to measure a reference spectrum. All gas mixtures were fed at a flow rate of 300 mL min^{-1}. All spectra were measured with a resolution of 4 cm^{-1} and with an accumulation of 100 scans.

3. Results

3.1. Structural properties

The XRD pattern of uncalcined precursor prepared by a mixture of $Al(NO_3)_3$ and anhydrous ethylenediamine is shown as the top curve of Fig. 1. The peaks of the uncalcined sample were identified as nordstrandite (JCPDS No. 24-0006), one of the four aluminum trihydroxide ($Al(OH)_3$) polymorphs [26]. After being calcined at 873 K for 3 h, the sample demonstrated distinct peaks assigned to γ-Al_2O_3 (JCPDS No. 29-0063). Fig. 1 also exhibits the XRD patterns of Ag/Al_2O_3 catalysts with different silver loadings, all of which presented the characteristic peaks of γ-Al_2O_3. No peaks indexed to silver species could be found when silver loadings were below 5 wt%, indicating its high dispersion. However, further increasing the silver content resulted in an appearance of peaks attributable to silver oxides, indicating aggregation of silver species.

As listed in Table 1, calcining the prepared nordstrandite resulted in notable increases in the surface area and the pore volume, while the pore diameter remained almost the same. It should

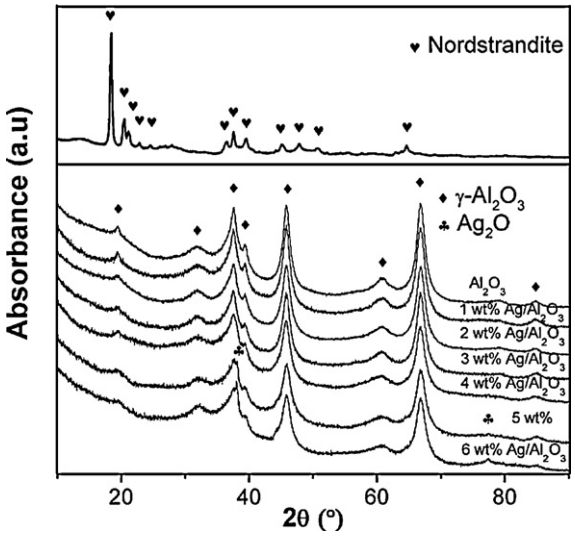

Fig. 1. XRD patterns of nordstrandite and Ag/Al_2O_3 catalysts with different silver loadings.

be noted that silver loading further increased the surface area, while the pore volume decreased. The catalysts with moderate silver loading content (3–5 wt%) exhibited the highest surface area, 302.7–303.4 m^2/g, indicating a favorable interaction between silver species and the support of γ-Al_2O_3.

The TEM images gave a visual understanding of the morphology and particle size distribution of the prepared samples (Fig. 2). The nordstrandite prepared by precipitation was in the form of irregular sheets with smooth surfaces (Fig. 2A). After calcination, plentiful pore structures clearly appeared on the surface and were conserved even after impregnation with the active component, which may contribute to the increase in surface area arising from the calcination process (Fig. 2B and C). In addition, Ag particles with diameter of around 15 nm could be observed uniformly distributed over 4 wt% Ag/Al_2O_3 (Fig. 2C).

3.2. Catalytic activity for NO_x reduction by ethanol and ammonia formation on Ag/Al_2O_3 catalysts

Fig. 3 displays the conversion of NO_x by ethanol, NH_3 yield, and N_2 selectivity over Ag/Al_2O_3 with different silver loadings. Over the whole temperature region of 473–823 K, increasing the silver content from 1 wt% to 2 wt% significantly enhanced the NO_x conversion, the latter of which exhibited NO_x conversion above 95% with a wide temperature window of 200 K (594–793 K). Increasing silver loading to 3 wt% further enhanced NO_x conversion in the low temperature region, while it decreased NO_x reduction at temperatures above 713 K. However, further increasing silver loading significantly decreased NO_x conversion in the high temperature region while only slightly enhancing the NO_x reduction at low temperatures.

As shown in Fig. 3C, the formation of NH_3 was also significantly enhanced when silver loading increased from 1 wt% to 2 wt%, while it gradually decreased when the silver loading continued to increase. Noticeably, ammonia was present over all the catalysts tested at temperatures above 548 K. Compared to the 2 wt% Ag/Al_2O_3 catalyst, 3 wt% Ag/Al_2O_3 showed a similar temperature range for 100% NO_x conversion, except that it was shifted toward lower temperature. However, the production of NH_3 on 3 wt% Ag/Al_2O_3 was much lower than that on the 2 wt% sample at temperatures above 600 K, exhibiting a high N_2 selectivity (Fig. 3B). Within a wide temperature range of 570–750 K, indeed, the 3 wt% Ag/Al_2O_3 showed almost the highest N_2 selectivity. Thus, the following experiments were performed on the sample of 3 wt% Ag/Al_2O_3.

A comparison of catalytic activity and NH_3 selectivity between our research and others in the literature is given in Table S1 [18,19,27,28]. Apparently, the catalysts prepared from nordstrandite in our research showed advantages in terms of lower T_{50} (temperature required for 50% NO_x conversion) and higher N_2 selectivity. However, NH_3 formation was a widespread phenomenon during HC-SCR over Ag/Al_2O_3 catalysts with different reductants, the amount of which varied with the catalysts used and reaction conditions.

Fig. S1 further shows the concentrations of NO, NO_2, N_2O, and NH_3 in the outlet gas during NO_x reduction by ethanol over 3 wt% Ag/Al_2O_3 at different temperatures. Sharp decreases in the concentration of NO and NO_2 were observed when the reaction temperature gradually increased to 600 K, which was accompanied by a gradual increase in NH_3 concentration. Over the temperature region of 600–700 K, NO_x were almost totally consumed while the amount of NH_3 went on increasing; whereas at temperatures above 700 K, NO appeared again and its concentration increased with increasing temperature. Within this temperature range, a decreased NH_3 concentration was observed simultaneously. The coexistence of NO_x and NH_3 indicated that the silver catalyst was not efficient for NH_3-SCR in the absence of promoters (such as H_2) over the tested temperature region, which was in agreement with the results of Kondratenko et al. [25] and Shimizu et al. [29]. As reported by Meunier et al. [8], it should be noted, however, that the presences of NO_2 and NH_3 during propene-SCR over Ag/Al_2O_3 in the absence of water vapor were mutually exclusive, i.e., NO_2 could be observed only when NH_3 was absent and vice versa, which is contrast to the data reported in the present work. This discrepancy may be possibly explained by differences in the nature of the reductant (propene vs ethanol) and reaction conditions (without water vapor vs with water vapor) employed in experiments. Indeed, the coexistence of NH_3 and NO_2 was also observed by Lee et al. [27] during ethanol-SCR over Ag/Al_2O_3 in the presence of water vapor.

Fig. 4 shows the influence of ethanol concentration on the NO_x conversion and the formation of ammonia over 3 wt% Ag/Al_2O_3 catalyst. When 783 ppm ethanol was introduced (giving a molar ratio of C/N around 2), the Ag/Al_2O_3 was not highly active for NO_x conversion, exhibiting a maximum value of 65% at 659 K, during which the highest concentration of ammonia (78 ppm) was observed at 763 K. Gradually increasing the ethanol concentration from 783 to 1252 ppm notably enhanced NO_x conversion at temperatures above 525 K, during which the same trend was also observed for the NH_3 and N_2 selectivities. Further increased feeding of ethanol slightly improved NO_x conversion at temperatures above 700 K, while the production of NH_3 was still significant over the whole temperature region. Miyadera [19] also adjusted the ethanol inlet concentration (C/N = 1.5–2.5) in ethanol-SCR over 2 wt% Ag/Al_2O_3 catalyst, and a higher C/N ratio gave higher NO_x conversion, N_2 selectivity, and NH_3 yield even without water.

Table 1
Structural parameters of nordstrandite and Ag/Al_2O_3 catalysts with different silver loadings derived from N_2 physisorption results.

Sample	BET surface area (m^2/g)	Pore volume (cm^3/g)	Pore diameter (nm)
Nordstrandite	180.5	0.22	3.82
Al_2O_3	242.0	0.42	3.82
1 wt% Ag/Al_2O_3	269.1	0.40	3.41
2 wt% Ag/Al_2O_3	289.4	0.38	3.40
3 wt% Ag/Al_2O_3	303.4	0.35	3.41
4 wt% Ag/Al_2O_3	303.3	0.32	3.40
5 wt% Ag/Al_2O_3	302.7	0.27	3.40
6 wt% Ag/Al_2O_3	271.3	0.25	3.40

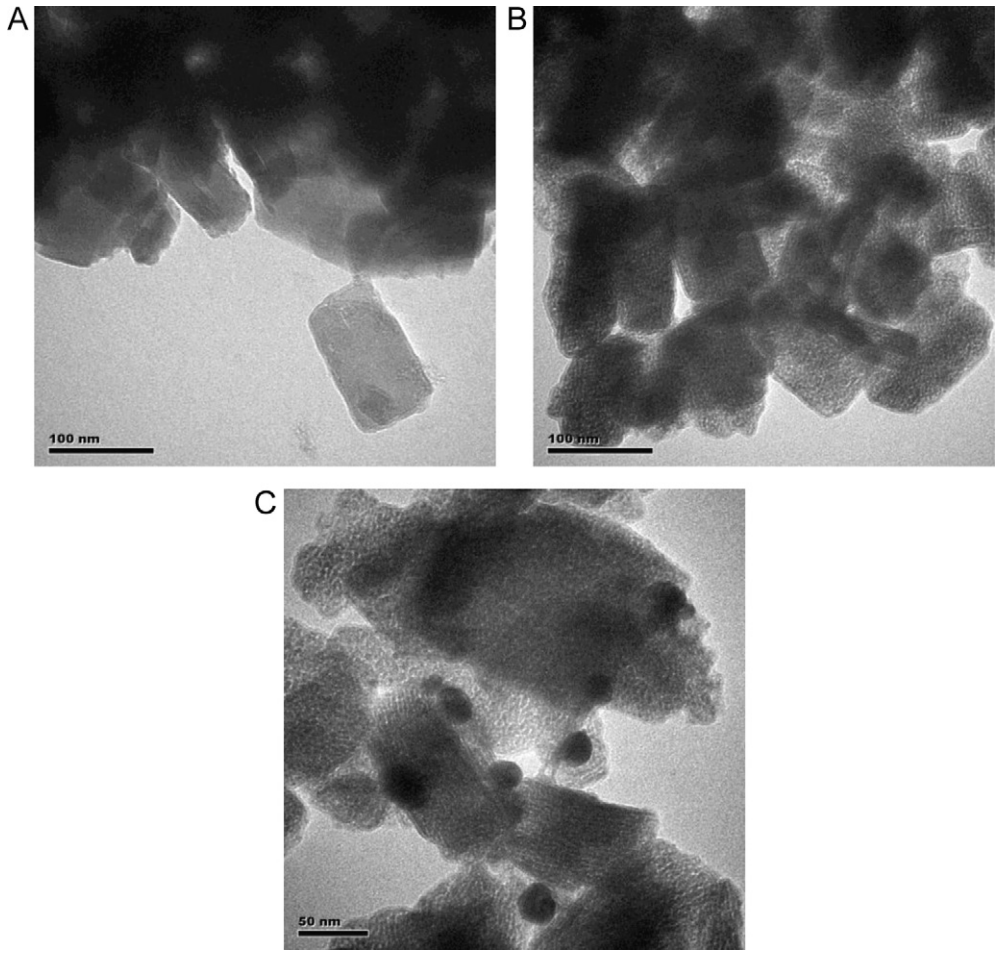

Fig. 2. TEM images of nordstrandite (A), Al_2O_3 (B), and 4 wt% Ag/Al_2O_3 (C).

It has been proposed that the presence of water vapor triggered the hydrolysis of –NCO formed during the HC-SCR process, and thus enhanced the production of NH_3 [19,23]. To highlight this issue, we compared NO_x conversion and NH_3 formation on 3 wt% Ag/Al_2O_3 with and without water vapor. As shown in Fig. S2A, the addition of water in the reaction gas slightly enhanced NO_x conversion at temperatures above 650 K. However, it should be noted that water vapor drastically increased the concentration of NH_3, particularly at temperatures above 550 K (giving a maximum of 166 ppm, 1.5 times higher than that in the absence of water vapor), which results in a decrease of N_2 selectivity (Fig. S2B). Noticeably, the formation of NH_3 was still observed even when water vapor was switched out from the inlet gas, suggesting that surface-adsorbed species formed during the reduction of NO_x by ethanol readily react with water to produce NH_3 (Fig. S2C).

3.3. The promotion of NO_x conversion by ammonia addition

The reduction of NO_x by ammonia over 3 wt% Ag/Al_2O_3 was also carried out in our research. Results given in Fig. S3A showed that the maximum conversion of NO_x was 17% at temperatures above 673 K in standard SCR, and even in fast SCR the maximum conversion was only around 25%, similar to the results reported by Richter et al. [24]. What's more, up to 175 ppm N_2O was formed even at the low temperature of 570 K during fast SCR, which is much higher than that detected during the ethanol-SCR process.

Furthermore, 150 ppm NH_3 was added into the inlet gas of the SCR of NO_x by ethanol over 3 wt% Ag/Al_2O_3 at 523 K, during which the concentration of NO_2 decreased 112 ppm (from 184 ppm to 72 ppm), as shown in Fig. 5. At the same time, the concentration of NO decreased about 30 ppm and that of N_2O remained almost the same (below 5 ppm). With the decreases of NO and NO_2 concentrations, the concentration of NH_3 in the outlet increased from 64 ppm to 123 ppm, giving a net change of 91 ppm considering the addition of 150 ppm NH_3 in the feed gas. These results suggest that further NO_x reduction occurred after NH_3 was introduced into the ethanol-SCR system. Assuming that the reaction among NO, NO_2 and NH_3 over Ag/Al_2O_3 follows the typical standard and/or fast NH_3-SCR process [2,5,30]:

$$4NH_3 + 4NO + O_2 \rightarrow 4N_2 + 6H_2O$$

$$2NH_3 + NO + NO_2 \rightarrow 2N_2 + 3H_2O$$

The theoretical consumption of NO should be equal to or higher than that of NO_2, while in our case, the decrease of NO was 73% lower than that of NO_2, clearly indicating the occurrence of a reaction pathway different to that of the NH_3-SCR process.

The role of NH_3 in the oxidation of ethanol over 3 wt% Ag/Al_2O_3 was further investigated (Fig. 6). At 498 K, adding NH_3 resulted in an increase of ethanol conversion from 45% to 54% (141 ppm decrease). Meanwhile, it should be noted that the concentration of acetaldehyde also increased about 120 ppm, indicating an enhancement of the partial oxidation of ethanol. As temperature increased, the enhancements of ethanol conversion and acetaldehyde formation induced by NH_3 addition gradually decreased, and disappeared above 598 K.

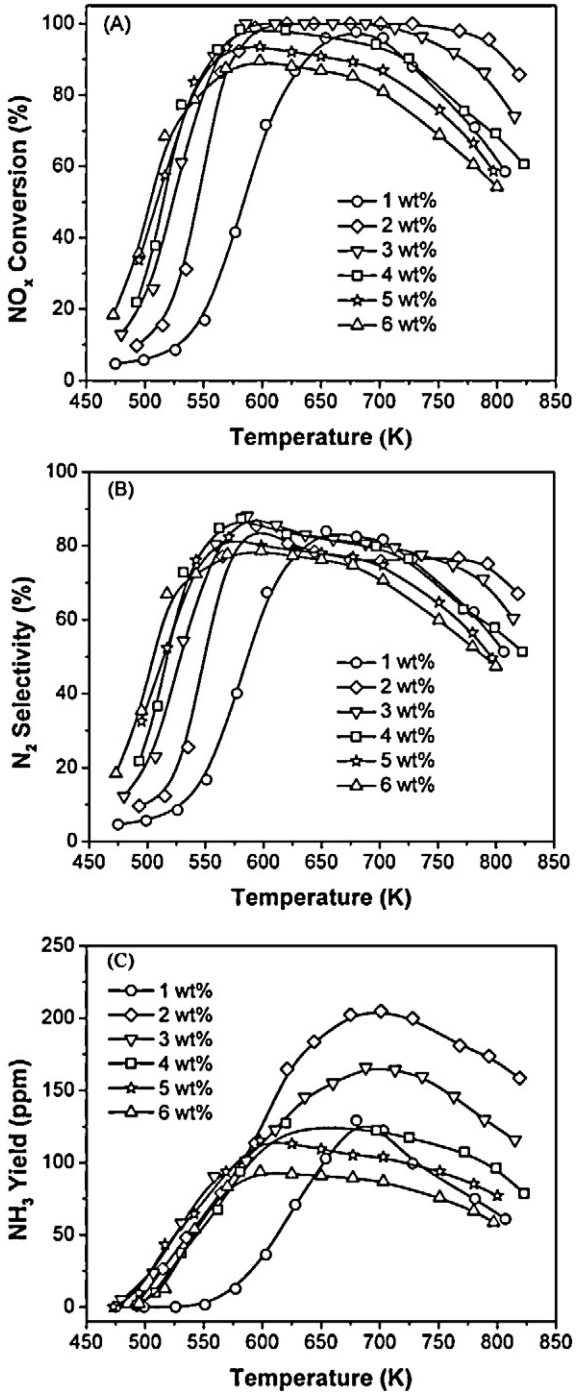

Fig. 3. NO_x conversion (A), N_2 selectivity (B), and NH_3 yield (C) for the SCR by C_2H_5OH over Ag/Al_2O_3 catalysts with different silver loading. Conditions: NO 800 ppm, C_2H_5OH 1565 ppm, O_2 10%, H_2O 10%, N_2 balance, GHSV: 50,000 h^{-1}.

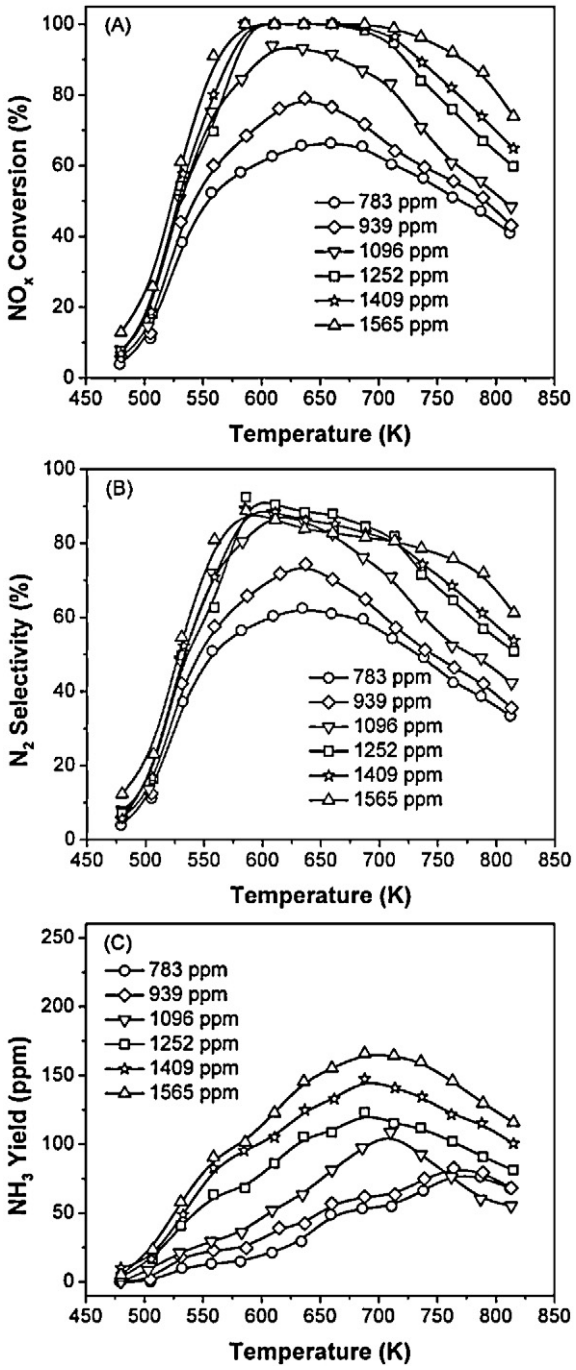

Fig. 4. NO_x conversion (A), N_2 selectivity (B), and NH_3 yield (C) for the SCR of NO_x over 3 wt% Ag/Al_2O_3 by different amount of C_2H_5OH. Conditions: NO 800 ppm, O_2 10%, H_2O 10%, N_2 balance, GHSV: 50,000 h^{-1}.

3.4. *In situ DRIFT studies*

At the heart of HC-SCR of NO_x over Ag/Al_2O_3 is the surface mechanism [1,13]. With this in mind, in situ DRIFTS measurements were performed to reveal the influence of NH_3 addition on the partial oxidation of ethanol and on its further reaction with $NO + O_2$ over 3 wt% Ag/Al_2O_3, with the result shown in Fig. 7 A. After exposing the catalyst to $C_2H_5OH + O_2$ at 548 K for 60 min, strong peaks at 1633, 1409 and 1338 cm^{-1} were clearly observed, which have been assigned to enolic species [21,31–33]. Over Ag/Al_2O_3, this surface species prefers to adsorb on or close to silver sites, exhibiting an intimate contact with the active phase. Surface acetate also formed during this process, giving the characteristic frequencies at 1570 and 1466 cm^{-1} [8,31,34]. Switching the feed gas to $NH_3 + O_2$ led to a gradual decrease in the intensity of enolic species, which was accompanied by the appearance of peaks at 2253 and 2233 cm^{-1}. Many studies have been devoted to the assignment of these two peaks, which have been attributed to isocyanate species (–NCO) and play a crucial role in HC-SCR over Ag/Al_2O_3 [1,13,35,36]. Meanwhile, it should be noted that the intensity of the acetate peaks hardly changed upon introduction of $NH_3 + O_2$, indicating its lower reactivity. As proposed by Yan et al. [21] recently, the enolic species bound on or close to

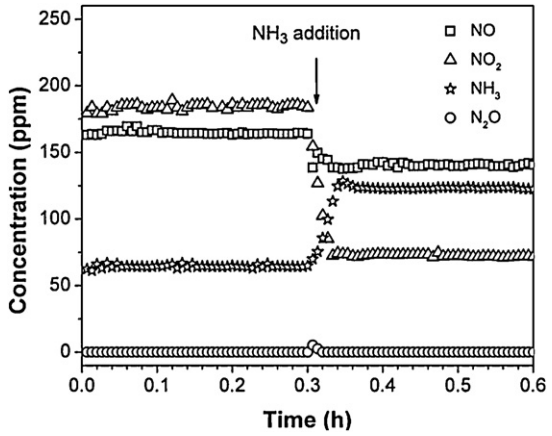

Fig. 5. The change of the concentration of nitrogen-containing gas composition in the outlet during the addition of 150 ppm NH_3 over 3 wt% Ag/Al_2O_3 at 548 K. Conditions: NO 800 ppm, O_2 10%, H_2O 10%, C_2H_5OH 1565 ppm, NH_3 150 ppm (when added), N_2 balance, GHSV: 50,000 h^{-1}.

Ag sites exhibits high activity for the formation of –NCO and thus contributes to the final product N_2 during the reduction of NO_x by ethanol over Ag/Al_2O_3. Acetate, as another species originating from the partial oxidation of ethanol over Ag/Al_2O_3, prefers to interact with Al sites, resulting in a lower activity for –NCO formation. In the present study, the same situation was also observed when the two species were exposed to $NH_3 + O_2$. In other words, the enolic species exhibits higher reactivity toward $NH_3 + O_2$ to form –NCO than acetate.

After 25 min, the gas flow was changed to $NO + O_2$, leading to a further increase of the intensity of –NCO peaks, reaching its maximum after another 5 min, and then gradually decreasing to a much lower level than that before the introduction of $NO + O_2$. At the same time, obvious significant consumption of enolic species was observed, contributing to the formation of –NCO. Finally, the intensity of –NCO peaks became weaker than that before the introduction of NO, indicating that the –NCO formed by NH_3 reacting with enolic species is also active for reaction with $NO + O_2$. In addition, peaks assigned to nitrates were observed at 1583 and 1302 cm^{-1} [31,37,38]. The appearance of a weak peak at around 2150 cm^{-1} indicates the formation of a small amount of –CN species [1,12].

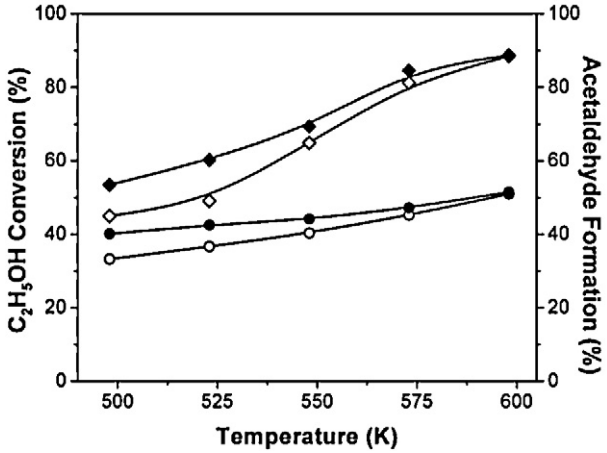

Fig. 6. The total conversions of ethanol (left axis) and the percentage of ethanol converted into acetaldehyde (right axis) in the presence of NH_3 (solid symbols) or in the absence of NH_3 (open symbols) over 3 wt% Ag/Al_2O_3. Conditions: NO 800 ppm, C_2H_5OH 1565 ppm, O_2 10%, H_2O 10%, NH_3 150 ppm (when added), N_2 balance, GHSV: 50,000 h^{-1}.

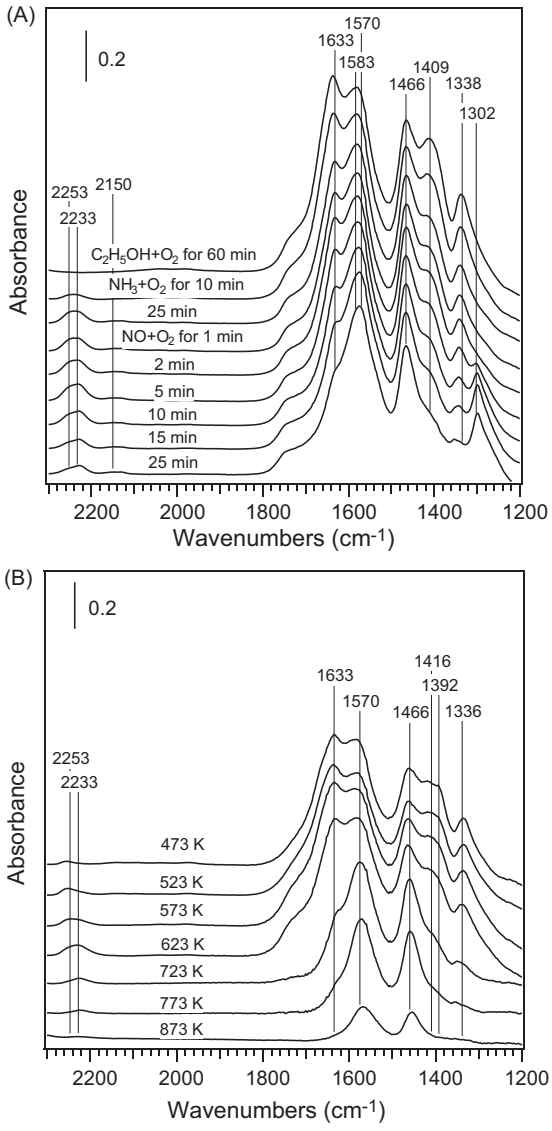

Fig. 7. Dynamic changes of in situ DRIFTS spectra over 3 wt% Ag/Al_2O_3 as a function of time in a flow of $NO + O_2$ at 573 K (A). Before measurement, the catalyst was pre-exposed to a flow of $C_2H_5OH + O_2$ for 60 min at 673 K and subsequently exposed to a flow of $NH_3 + O_2$ for 25 min. In situ DRIFTS spectra of adsorbed species on 3 wt% Ag/Al_2O_3 in steady states in a flow of $C_2H_5OH + O_2 + NH_3$ at different temperatures (B). Conditions: NO 800 ppm, C_2H_5OH 1565 ppm, NH_3 150 ppm,O_2 10%, N_2 balance.

Fig. 7B further shows the in situ DRIFTS spectra of 3 wt% Ag/Al_2O_3 during the reaction of $C_2H_5OH + NH_3 + O_2$ at steady state within the temperature range of 473–873 K. Similar to our previous result in the absence of NH_3 [32,33], the enolic species was predominant within the low temperature range of 473–623 K, while acetate was dominant at temperatures above 623 K. In contrast, the peaks assignable to –NCO were observed over the whole temperature range during the partial oxidation of ethanol in the presence of NH_3, indicating a critical role of NH_3 in –NCO formation in this case.

As identified in Fig. S2C, surface adsorbed species formed during the reduction of NO_x by ethanol readily react with water to produce NH_3. To reveal the species contributing to the formation of NH_3, a similar experiment was performed by in situ DRIFTS (Fig. 8). After 60 min steady SCR reaction in a flow of $C_2H_5OH + NO + O_2$ at 548 K, the peak at 2233 cm^{-1} ascribed to –NCO species was stabilized (Fig. 8A). The intensity of –NCO peaks exhibited a slight increment due to further transformation from enolic species during

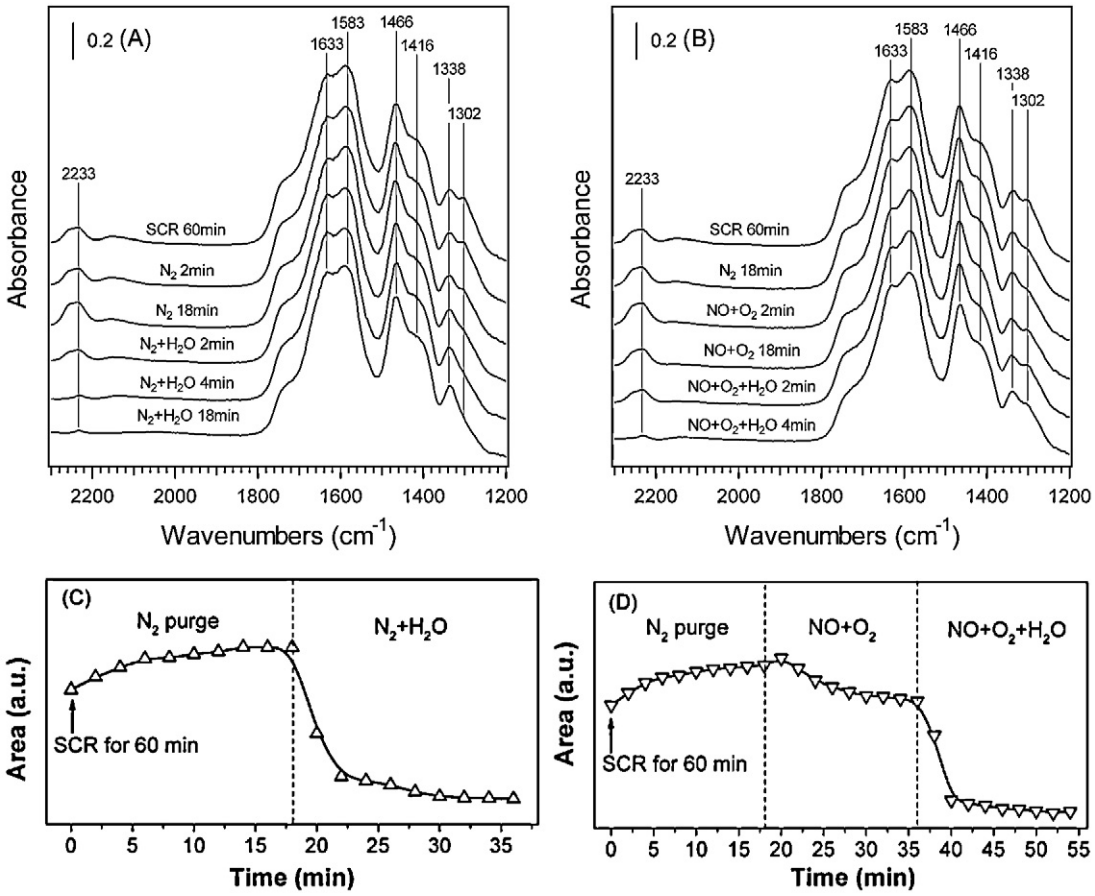

Fig. 8. Dynamic changes of in situ DRIFTS spectra over 3 wt% Ag/Al_2O_3 as a function of time in N_2 purging followed by exposure to water vapor balanced by N_2 (A) and N_2 purging followed by exposure to $NO + O_2$ and $NO + O_2 + H_2O$ in sequence (B) at 548 K; (C) and (D): time dependence of the corresponding integrated areas of the peaks of –NCO in the cases of (A), and (B), respectively. Before measurement, the catalyst was pre-exposed to a flow of $C_2H_5OH + NO + O_2$ for 60 min at 548 K. Conditions: NO 800 ppm, C_2H_5OH 1565 ppm, O_2 10%, H_2O 1%, N_2 balance.

N_2 purging for 18 min. Once 1% H_2O was introduced, the peak area of –NCO species (Fig. 8C) was reduced sharply in 4 min, and almost disappeared in 10 min, certifying high activity of –NCO toward H_2O. Actually, the consumption of –NCO in a feed of $NO + O_2 + H_2O$ was close to that of H_2O carried by N_2 (Fig. 8B and D). This result indicates that the reaction rate of –NCO hydrolysis is much higher than that of the reaction between –NCO and $NO + O_2$ (or surface nitrates), which is in good agreement with the results of Bion et al. [12] and Tamm et al. [23].

3.5. NO_x reduction by ethanol over Ag/Al_2O_3 + Cu based catalyst

In consideration of the inactivity of the Ag/Al_2O_3 catalyst for NH_3-SCR, an additional oxidation catalyst might be needed to decrease NH_3 emission from the ethanol-SCR process. Previous studies revealed that Cu-based catalysts were active for selective catalytic oxidation (SCO) of NH_3 to produce N_2 [39]. With this in mind, a combination of Ag/Al_2O_3 with Cu/TiO_2 (or Cu/Al_2O_3) was employed in NO_x reduction by ethanol, giving 100% NO_x conversion between 575 and 725 K. As shown in Fig. S4, the dual-bed system of $Ag/Al_2O_3 + Cu/TiO_2$ decreased the NH_3 concentration from 165 ppm to 20 ppm at 700 K while the N_2 selectivity increased up to 96%, more effectively than Ag/Al_2O_3 or the system of $Ag/Al_2O_3 + Cu/Al_2O_3$. The above result is comparable to the results of He et al. [40] and other dual-bed systems, such as a combination of Ag/Al_2O_3 and Cu-ZSM5 catalysts [28]. However, the combination of SCR and NH_3-SCO catalysts could not completely eliminate the NH_3 formed. Thus, more efforts are needed to eliminate the potential hazard of NH_3 emission.

4. Discussion

The Ag/Al_2O_3 catalysts prepared using nordstrandite as a precursor of alumina exhibited excellent activity for reduction of NO_x by ethanol. With a moderate silver loading (2–3 wt%), NO_x conversion above 95% was obtained within a wide temperature window of 200 K. It has been widely accepted that the surface property of γ-Al_2O_3 relating to hydroxyl groups (–OH) is fundamental in governing the dispersion of the supported active phases, and thus contributes to the reactivity of the final catalyst [41–43]. Nordstrandite, as one of the four aluminum trihydroxide ($Al(OH)_3$) polymorphs, contains more abundant –OH groups than γ-Al_2O_3. With this in mind, it can be expected that an abundance of anchoring sites are available for dispersion of an active phase if nordstrandite is be used as a precursor of the support. Such a feature may contribute to the high activity for NO_x reduction of Ag/Al_2O_3 prepared from nordstrandite in our research. Calcining the sample of nordstrandite results in the formation of γ-Al_2O_3 (Fig. 1), the occurrence of which also results in an increase in the specific surface area (Table 1). This tendency is more noticeable when the samples with moderate silver loadings are calcined, possibly suggesting the formation of a strong interaction between silver species and the support during the phase transformation of the nordstrandite. Generally, a strong interaction of the active phase of silver

with the support is beneficial for HC-SCR of NO_x over Ag/Al_2O_3 [17,21,44].

During this process, however, the unexpected product of ammonia was formed, the amount of which varied with reaction conditions and silver loadings. A decrease of the concentration of ethanol employed significantly lowered the release of ammonia at the expense of NO_x conversion, although not enough to eliminate the NH_3 production.

As confirmed by previous studies [12,35,45], the surface –NCO species possesses high reactivity toward $NO + O_2$ to form N_2, and thus contributes to NO_x reduction by hydrocarbons and oxygenated hydrocarbons over Ag/Al_2O_3. This species also exhibits even much higher activity toward water vapor to produce NH_3 [12,23]. The release of NH_3 during ethanol-SCR in the presence of H_2O was mainly attributed to the hydrolysis of –NCO species over Ag/Al_2O_3, which has been identified by activity testing and FTIR analysis (Figs. 4 and 7). During ethanol-SCR over Ag/Al_2O_3, the final products of ethanol oxidation are H_2O and CO_2. With this in mind, it is reasonable that, even in dry feed gas, NH_3 was also produced during the ethanol-SCR (Fig. S2A).

As a reducing species of nitrogen, NH_3 has been considered to have the potential to react with NO_x to produce N_2 during HC-SCR over Ag/Al_2O_3, following the mechanism of NH_3-SCR [18,28,46]. By adding NH_3 into the feed gas of ethanol-SCR over Ag/Al_2O_3 (Fig. 5), however, the consumption of NO was much lower than that of NO_2, which is not in agreement with the theoretical value based on the typical NH_3-SCR processes, strongly suggesting the occurrence of a reaction pathway quite different to that of NH_3-SCR. Further evidence can be found when NH_3 served as a reductant: the fed NO_x was mainly converted to N_2O over Ag/Al_2O_3 (Fig. S3B), significantly different from ethanol-SCR. During ethanol-SCR over 3 wt% Ag/Al_2O_3 (Fig. S1), meanwhile, the co-existence of NO and NH_3 was observed at temperatures above 673 K. Moreover, at temperatures below 573 K, NO, NO_2 and NH_3 are all present in the outlet gas, and their concentrations meet the requirement for fast-SCR [47,48]. The above results further demonstrated the inactivity of Ag/Al_2O_3 for the NH_3-SCR reaction.

Interestingly, the presence of NH_3 enhanced the partial oxidation of ethanol over Ag/Al_2O_3 (Fig. 6), particularly at the light-off temperature for the ethanol-SCR reaction. As a result, a higher concentration of CH_3CHO was measured in the gas phase. During the hydrocarbon oxidation, the produced CH_3CHO readily isomerizes to ethanol [49]. On the Ag/Al_2O_3 surface, CH_3CHO may mainly be present as enolic species, by isomerization to enol and then hydrogen extraction [46]. In organic synthesis, it is well known that aldehydes and their isomers of enols easily react with ammonia to produce oxime, giving a structure of –CH = N(OH), which possibly occurs on the surface of Ag/Al_2O_3 during the ethanol-SCR. The oxime then transforms to amide via Beckmann rearrangement, from which –NCO species can be produced by dehydrogenation [8,46,50]. Further in situ DRIFTS results presented here reveal that NH_3 can react with surface enolic species to form –NCO species (Fig. 7), the reaction pathway of which can be proposed as follows:

$$NH_3 + \text{enolic species (and/or } CH_3CHO) \rightarrow \text{R-CH} = \text{NOH} \rightarrow \text{R-CO-NH}_2 \rightarrow \text{–NCO}$$

Based on all the observations presented in this study and available literature reports, plausible reaction pathways for ethanol-SCR over Ag/Al_2O_3 are proposed, as shown in Scheme 1. In a typical reaction process, partial oxidation of ethanol results in the formation of enolic species and acetate. The surface enolic species can react with $NO + O_2$ and/or NO to produce –NCO species, possibly via the formation of organic nitroso and nitro compounds. Further reaction between –NCO and $NO + O_2$ results in the formation of the final product of N_2. The acetate also participates in this process, while its lower activity toward $NO + O_2$ (and/or NO) results in its minor role in –NCO formation, and thus in the NO_x reduction process.

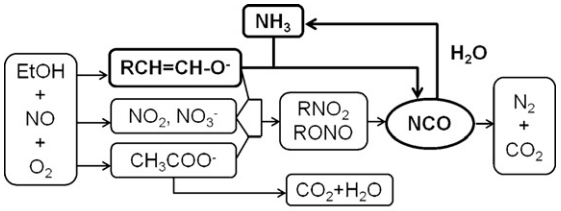

$NH_3 + RCH{=}CH{-}O^- \rightarrow R{-}CH{=}NOH \rightarrow R{-}CO{-}NH_2 \rightarrow {-}NCO$

Scheme 1. The mechanism of the SCR of NO_x by C_2H_5OH over Ag/Al_2O_3.

Water vapor is inevitably present in the ethanol-SCR system, by addition and/or as produced from the oxidation of ethanol over Ag/Al_2O_3. On the surface of Ag/Al_2O_3, water vapor triggers the hydrolysis of –NCO species to produce NH_3, the latter of which in turn can react with enolic species to form –NCO, providing a new and cyclic pathway during the NO_x reduction by ethanol.

If compared with the reaction of –NCO with $NO + O_2$ and with water vapor over Ag/Al_2O_3, we can estimate that the reaction rate of the latter is much higher than that of the former. Such a high reaction rate of –NCO hydrolysis may result in a significant decrease in N_2 selectivity for ethanol-SCR over Ag/Al_2O_3. However, as shown in Fig. S2B, the practical N_2 selectivity during NO_x reduction by ethanol does not decrease so much, which in turn demonstrates the crucial role of NH_3 in NO_x reduction by cyclic reaction with enolic species. Yet, it should be pointed out that it is difficult to do accurate measurements on the contribution of NH_3 for NO_x reduction by ethanol, with consideration of the following facts. The fact that NH_3 was still released even in ethanol-SCR with dry feed gas, indicates that it is hard to create reaction conditions without the formation of NH_3. In the absence of NO_x, the contribution of NH_3 to the partial oxidation of ethanol is limited, while this contribution will be prompted in the presence of NO_x.

5. Conclusions

Ammonia was inevitably produced over Ag/Al_2O_3 catalysts during the SCR of NO_x by ethanol, the release of which derived from the high reaction rate of –NCO hydrolysis. Ammonia also participates in NO_x reduction during ethanol-SCR while it cannot be accounted for by the typical NH_3-SCR process. Ammonia originating from the hydrolysis of –NCO species can in turn react with enolic species, to produce –NCO. The reaction between ammonia and enolic species thus creates a cyclic pathway for NO_x reduction by ethanol, which may guarantee the high efficiency of the ethanol-SCR system.

Acknowledgments

This work was supported by the National Natural Science Foundation of China (21177142, 20973193) and the National High Technology Research and Development Program of China (863 Program, 2013AA065301).

Appendix A. Supplementary data

Supplementary data associated with this article can be found, in the online version, at http://dx.doi.org/10.1016/j.apcatb.2013.01.048.

References

[1] R. Burch, J.P. Breen, F.C. Meunier, Appl. Catal. B 39 (2002) 283.
[2] M.A. Gómez-García, V. Pitchon, A. Kiennemann, Environ. Int. 31 (2005) 445.
[3] Z. Liu, S. Ihl Woo, Catal. Rev. 48 (2006) 43.
[4] S. Roy, M.S. Hegde, G. Madras, Appl. Energy 86 (2009) 2283.
[5] P. Granger, V.I. Parvulescu, Chem. Rev. 111 (2011) 3155.
[6] F. Poignant, J.L. Freysz, M. Daturi, J. Saussey, Catal. Today 70 (2001) 197.
[7] K. Sato, T. Yoshinari, Y. Kintaichi, M. Haneda, H. Hamada, Appl. Catal. B 44 (2003) 67.
[8] F.C. Meunier, J.P. Breen, V. Zuzaniuk, M. Olsson, J.R.H. Ross, J. Catal. 187 (1999) 493.
[9] J. Li, J. Hao, L. Fu, T. Zhu, Z. Liu, X. Cui, Appl. Catal. A 265 (2004) 43.
[10] Y. Ukisu, T. Miyadera, A. Abe, K. Yoshida, Catal. Lett. 39 (1996) 265.
[11] K.A. Bethke, H.H. Kung, J. Catal. 172 (1997) 93.
[12] N. Bion, J. Saussey, M. Haneda, M. Daturi, J. Catal. 217 (2003) 47.
[13] H. He, Y.B. Yu, Catal. Today 100 (2005) 37.
[14] K.-I. Shimizu, A. Satsuma, Phys. Chem. Chem. Phys. 8 (2006) 2677.
[15] Y.B. Yu, X.P. Song, H. He, J. Catal. 271 (2010) 343.
[16] V.I. Pârvulescu, B. Cojocaru, V. Pârvulescu, R. Richards, Z. Li, C. Cadigan, P. Granger, P. Miquel, C. Hardacre, J. Catal. 272 (2010) 92.
[17] X. She, M. Flytzani-Stephanopoulos, J. Catal. 237 (2006) 79.
[18] T. Miyadera, Appl. Catal. B 16 (1998) 155.
[19] T. Miyadera, Appl. Catal. B 13 (1997) 157.
[20] F. Can, A. Flura, X. Courtois, S. Royer, G. Blanchard, P. Marecot, D. Duprez, Catal. Today 164 (2011) 474.
[21] Y. Yan, Y.B. Yu, H. He, J.J. Zhao, J. Catal. 293 (2012) 13.
[22] M.L. Unland, J. Phys. Chem. 77 (1973) 1952.
[23] S. Tamm, H.H. Ingelsten, A.E.C. Palmqvist, J. Catal. 255 (2008) 304.
[24] M. Richter, R. Fricke, R. Eckelt, Catal. Lett. 94 (2004) 115.
[25] E.V. Kondratenko, V.A. Kondratenko, M. Richter, R. Fricke, J. Catal. 239 (2006) 23.
[26] R.A.V. Nordstrand, W.P. Hettinger, C.D. Keith, Nature 177 (1956) 713.
[27] J.H. Lee, S.J. Schmieg, S.H. Oh, Appl. Catal. A 342 (2008) 78.
[28] M.K. Kim, P.S. Kim, J.H. Baik, I.-S. Nam, B.K. Cho, S.H. Oh, Appl. Catal. B 105 (2011) 1.
[29] K.-I. Shimizu, A. Satsuma, Appl. Catal. B 77 (2007) 202.
[30] P.G. Savva, C.N. Costa, Catal. Rev. 53 (2011) 91.
[31] Y.B. Yu, H. He, Q.C. Feng, H.W. Gao, X. Yang, Appl. Catal. B 49 (2004) 159.
[32] Y.B. Yu, H.W. Gao, H. He, Catal. Today 93–95 (2004) 805.
[33] Y.B. Yu, H. He, Q.C. Feng, J. Phys. Chem. B 107 (2003) 13090.
[34] K.-I. Shimizu, J. Shibata, H. Yoshida, A. Satsuma, T. Hattori, Appl. Catal. B 30 (2001) 151.
[35] S. Chansai, R. Burch, C. Hardacre, J. Breen, F. Meunier, J. Catal. 276 (2010) 49.
[36] S. Chansai, R. Burch, C. Hardacre, J. Breen, F. Meunier, J. Catal. 281 (2011) 98.
[37] S. Kameoka, Y. Ukisu, T. Miyadera, Phys. Chem. Chem. Phys. 2 (2000) 367.
[38] K.-I. Shimizu, A. Satsuma, T. Hattori, Appl. Catal. B 25 (2000) 239.
[39] X.P. Song, C.B. Zhang, H. He, Chin. J. Catal. 29 (2008) 524.
[40] S. He, C. Zhang, M. Yang, Y. Zhang, W. Xu, N. Cao, H. He, Sep. Purif. Technol. 58 (2007) 173.
[41] C. Morterra, G. Magnacca, Catal. Today 27 (1996) 497.
[42] M. Digne, P. Sautet, P. Raybaud, P. Euzen, H. Toulhoat, J. Catal. 226 (2004) 54.
[43] M. Digne, P. Sautet, P. Raybaud, P. Euzen, H. Toulhoat, J. Catal. 211 (2002) 1.
[44] R. Zhang, S. Kaliaguine, Appl. Catal. B 78 (2008) 275.
[45] F. Thibault-Starzyk, E. Seguin, S. Thomas, M. Daturi, H. Arnolds, D.A. King, Science 324 (2009) 1048.
[46] P.S. Kim, M.K. Kim, B.K. Cho, I.-S. Nam, J. Catal. 292 (2012) 44.
[47] M. Koebel, G. Madia, F. Raimondi, A. Wokaun, J. Catal. 209 (2002) 159.
[48] E. Tronconi, I. Nova, C. Ciardelli, D. Chatterjee, M. Weibel, J. Catal. 245 (2007) 1.
[49] C.A. Taatjes, N. Hansen, A. McIlroy, J.A. Miller, J.P. Senosiain, S.J. Klippenstein, F. Qi, L.S. Sheng, Y.W. Zhang, T.A. Cool, J. Wang, P.R. Westmoreland, M.E. Law, T. Kasper, K. Kohse-Hoinghaus, Science 308 (2005) 1887.
[50] E. Joubert, X. Courtois, P. Marecot, C. Canaff, D. Duprez, J. Catal. 243 (2006) 252.